Stable isotopic signatures of fossilised rodent teeth: climate change and faunal response in south-eastern Australia between 49 – 14 ka

Thesis submitted in accordance with the requirements of the University of Adelaide for an Honours Degree in Geology

Tiah Louise Bampton

November 2018

THE UNIVERSITY of ADELAIDE

STABLE ISOTOPIC SIGNATURES OF FOSSILISED RODENT TEETH: CLIMATE CHANGE IN SOUTH-EASTERN AUSTRALIA DURING THE LATE QUATERNARY AND FAUNAL RESPONSE

STABLE ISOTOPIC SIGNATURES OF FOSSILISED RODENT TEETH

ABSTRACT

The stable carbon ($\delta^{13}C$) and oxygen ($\delta^{18}O$) isotopic composition of bioapatite from fossilised mammalian tooth material is a well-established proxy for the reconstruction of palaeovegetation and palaeoclimate. The use of small mammals, in particular rodents, has been overlooked in the past for such studies. High abundances of fossilised rodent remains deposited by avian predators in cave deposits, such as Blanche Cave in the Naracoorte Caves World Heritage Area (NCWHA), gives researchers easy access to fossil materials, to which a temporal scale of climate and vegetation change can be reconstructed.

$\delta^{18}O$ and $\delta^{13}C$ analyses were performed on crushed incisors of three species of *Pseudomys (P. auritus, P. australis and P. shortridgei)* over the upper 27 layers from Blanche Cave, NCWHA. The relative abundances of the three species were collected from each layer and compiled into climatic-stratigraphic units: pre-glaciation (layers 27-25), early-glaciation (layers 24-20), Last Glacial Maximum (layers 19-15) and deglaciation (layers 13-1). The carbonate bound component of the bioapatite was analysed for $\delta^{13}C$ and $\delta^{18}O_{CO3,}$ as well as the additional analysis of phosphate bound oxygen ($\delta^{18}O_{PO4}$) using isotope ratio mass spectrometry. Isotopic signatures from $\delta^{13}C$ and $\delta^{18}O$ were used to reconstruct palaeoclimate and palaeovegetation over the four climatic-stratigraphic units, which were compared to existing palaeoclimate studies. As rodents are commonly abundant in fossil deposits, they have the potential of being used to determine climatic and vegetation change associated with extinction events, such as the megafauna extinction in Australia.

KEYWORDS

Stable isotopes, rodent, climate, late Quaternary, Naracoorte Caves, Blanche Cave, palaeoecology, Pseudomys

TABLE OF CONTENTS

Abstract i
Keywords i
List of Figures and Tables 2
Introduction 3
Geological Setting/Background 6
Geological Setting 6
Background 10
Methods 13
Results 16
Sedimentation Chronology 16
Relative Abundance of Fossil Teeth 16
Carbonate Isotope Variability 18
Phosphate $\delta^{18}O$ Variability 19
$\delta^{13}C$ vs $\delta^{18}O_{PO4}$ 22
Discussion 23
Isotopic Interpretations 23
Climatic Reconstruction 25
Species Response to Climate 28
Future Studies 30
Conclusion 30
Acknowledgments 31
References 31
Appendix A: Laboratorial Methods 35
Appendix B: Isotope Data 39
Appendix C: Relative Abundance Data 42

LIST OF FIGURES AND TABLES

Figure 1: a) Image of *Pseudomys australis*, common name: Plains Mouse (Francis, 2017) b) Image of *Pseudomys shortridgei*, common name: Heath Mouse (Paul, 2017). 6
Figure 2: a) Location of the Naracoorte Cave World Heritage Area (NCWHA), South-eastern South Australia. Map adapted from Macken, & Reed, (2013). b) Cave map of Blanche Cave with the excavation site from which the sample of this study were previously obtained. Map supplied by E. Reed. 8
Figure 3: Stratigraphic sequence of the first 27 layers of Blanche Cave excavation site, Naracoorte Caves World Heritage Area (NCWHA). Depth is approximately the first metre below cave ground surface. Mean ages for each layer obtained from Macken et al. (2013). The layers are divided into climatic-stratigraphic units; unit 1 – pre-glaciation (layers 27-25), unit 2 – early glaciation (layers 24-20), unit 3 – Last Glacial Maximum (layers 15-19) and unit 4 – deglaciation (layers 13-1). Photo taken by Steve Bourne. 9
Figure 4: Plot of the relative abundance (%), determined by the number of specimens (NISP) from fossilised lower jaws (dentaries), obtained from the Blanche Cave excavation site. The three species of *Pseudomys* (*P auritus*, *P. australis* and *P. shortridgei*) were plotted against the stratigraphic layers in the Blanche Cave excavation site and the age in years before present (years B. P.). The age for layer 14 has been excluded from the above figure as this layer has been reworked. Mean ages obtained from Macken et al. (2013). 17
Figure 5: Relative abundance (%), determined from the number of specimens (NISP) of fossilised dentaries from Blanche Cave for three species of *Pseudomys* (*P. auritus, P. australis* and *P. shortridgei),* plotted against the climatic-stratigraphic units; unit 1 – pre-glaciation (layers 27-25), unit 2 – early glaciation (layers 24-20), unit 3 – Last Glacial Maximum (layers 19-15) and unit 4 – deglaciation (layers 13-1), and age in years before present (years B. P.). Mean ages obtained from Macken et al. (2013). 18
Figure 6: Plots of stable isotope data from fossilised incisors of three species of *Pseudomys* (*P auritus*, *P. australis* and *P. shortridgei*) analysed by an Isotope Ratio Mass Spectrometer (IRMS), over stratigraphic layers in the Blanche Cave excavation site, and age in years before present (years B. P.). The age for layer 14 has been excluded from the above figure as this layer has been reworked. Mean ages obtained from Macken et al. (2013). a) $\delta^{13}C$ values in percent per mil (‰) of both tooth and diet signatures for the three *Pseudomys* species. b) $\delta^{18}O_{CO3}$ values (‰) of the carbonate bound oxygen from the tooth of the three *Pseudomys* species. c) $\delta^{18}O_{PO4}$ values (‰) of the phosphate bound oxygen from the tooth of the three *Pseudomys* species..... 21
Figure 7: Plot of $\delta^{13}C$ (‰) against $\delta^{18}O_{PO4}$ (‰) for the three *Pseudomys* species (*P. auritus, P. australis* and *P. shortridgei*). The points displayed are the data obtained from each species over the 27 layers of Blanche Cave Excavation Site, Naracoorte Caves World Heritage Area. The layers have been colour coded into climatic-stratigraphic units; unit 1 – pre-glaciation (layers 27-25), unit 2 – early glaciation (layers 24-20), unit 3 – Last Glacial Maximum (layers 19-15) and unit 4 – deglaciation (layers 13-1). 22

INTRODUCTION

Evidence of widespread extinction of megafauna in the Late Quaternary has been seen on all continents, excluding Antarctica (Trueman et al., 2005). The cause of extinction for these large vertebrates (>40kg in adolescents) in Australia has been greatly debated for over a century (Roberts et al., 2001; Saltré et al., 2016). There are three main hypotheses in debate; the 'Blitzkrieg model', namely rapid overkill of megafauna by human colonisers, modifications of the habitat caused by anthropological processes such as firing the landscape, and finally, palaeoecological changes in which climate change is the main driving force (Trueman et al., 2005). Resolving these questions requires a combination of evidence for biodiversity loss, high quality records of climate change and a detailed knowledge of human arrival and activity in order to objectively asses these hypotheses.

Fossil records have been useful in determining climates of the past as well as changes in biodiversity through time, where the presence of particular taxa provides information on possible climatic and environmental conditions. However, the interpretation of fossil assemblages as climate proxies alongside the investigation of the causation of biodiversity change presents a circularity which is hard to resolve without independent climate evidence (Clementz, 2012). In this context, the use of stable isotopes of oxygen and carbon within the fossil record have become a useful tool in developing habitat and palaeoclimatic records.

Bioapatite records the isotopic composition of carbon and oxygen from an individual throughout its life (Passey & Cerling, 2002). The isotopic carbon component in herbivores records consumption of C_4 or C_3 plants (Brookman & Ambrose, 2013), which can be used to infer palaeovegetation as well as dietary strategies among

individual populations (Gehler et al., 2012). Changes in the $\delta^{13}C$ of vegetation reflect a response to water stress in C_3 plants, where a higher $\delta^{13}C$ correlates to low levels of precipitation (Falster et al., 2018) or shifts in the relative abundance of C_3 and C_4 (Gehler et al., 2012). The oxygen isotopic signature of tooth bioapatite reflects an individual's body water, which is sourced from local drinking water or diet via leaf water (Montanari et al., 2013). Oxygen isotopes in water are a widely applied tracer of past and present climate and hydrological variability, due to a sensitivity to phase changes (evaporation/condensation) and partitioning of water in the environment (Gehler et al., 2012). The analysis of these isotopes in bioapatite from fossilised remains is the basis of this study.

The Naracoorte Caves World Heritage Area (NCWHA) is in the south-eastern region of South Australia and consists of 26 known caves (Figure 1a). These caves provide a stable condition for long term preservation of an extensive record of flora and fauna, ranging from megafauna to small vertebrates, from the Middle Pleistocene to the Holocene (Reed & Bourne, 2000). The research that has been conducted on the fossil assemblages from the NCWHA has made a significant impact on our understanding of the faunal communities through the Middle to Late Pleistocene (Prideaux et al., 2007). This includes the effect of change in climate, as well as the taxonomy and systematics of both extinct and extant fauna of south-eastern South Australia (Macken & Reed, 2013).

The Naracoorte Caves small mammal deposits show a high dominance of rodents, where their high abundance and diversity makes them ideal for palaeontological studies (Macken & Reed, 2013). In this study, the main focus was on the family Muridae (rodents), specifically the genus *Pseudomys* which are endemic to Australia and were

commonly found in the south-eastern region of South Australia during the Late Pleistocene. The three species in this study include two extant species: *Pseudomys australis* and *P. shortridgei* (Figure 1), and an extinct species: *P. auritus* (extinct since European settlement). The specimens for this study were previously collected from Blanche Cave in the NCWHA. Incisors were sampled from identified lower jaws of each species for stable isotope analysis by mass spectrometry. The resulting signatures were used to infer the palaeoclimate change over four units, spanning approximately 49-14 ka (Macken et al., 2013). The units were segmented by different pre-established environmental states; pre-glaciation, early glaciation, the Last Glacial Maximum (LGM), and deglaciation. From this analysis, the dietary preference and vegetation change through time was shown in the stable isotopic signature of carbon, and changes in body water signatures from oxygen isotopes represented the relative humidity or aridity of the Late Pleistocene. NCWHA displayed evidence of long-term resistance of the faunal communities through climatic change in the area (Macken et al., 2012). Relative abundance between the three species of *Pseudomys* (*Pseudomys auritus, P. australis* and *P. shortridgei*) was also compared to the climatic interpretations made. This comparison can help to understand how communities react to changes in climate (Macken et al., 2012).

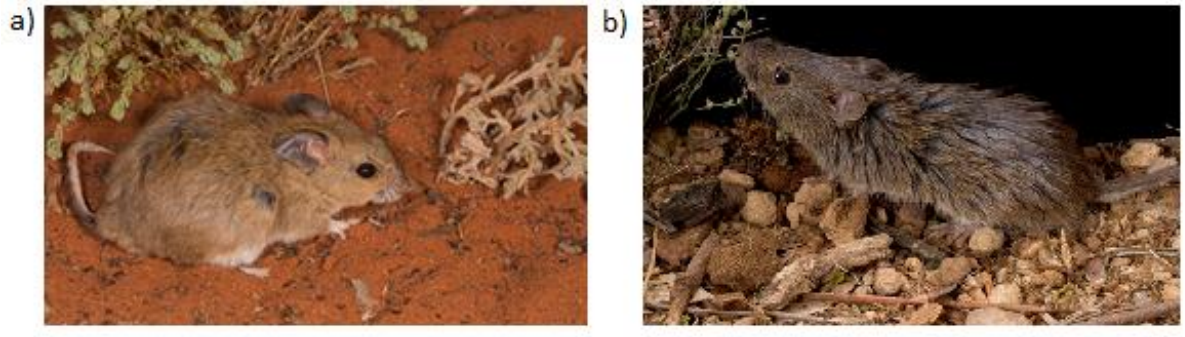

Figure 1: a) Image of *Pseudomys australis*, common name: Plains Mouse (Francis, 2017) b) Image of *Pseudomys shortridgei*, common name: Heath Mouse (Paul, 2017).

GEOLOGICAL SETTING/BACKGROUND

Geological Setting

The Naracoorte Caves are situated in the uplifted section of the Eocene to Miocene aged fossiliferous Gambier Limestone that underlies the south-eastern region of South Australia (Figure 2a) (White & Webb, 2015). Phreatic dissolution of the limestone in the early Pleistocene led to the development of passages that connect large solution chambers and collapsed domes (White & Webb, 2015). Overlying this extensive cave system is the East Naracoorte Ridge, which consists of Pliocene and Pleistocene dunes (Forbes & Bestland, 2007). The caves opened during the early to middle Pleistocene (White & Webb, 2015) via solution pipe development and collapse of roof window entrances which allowed sediments to enter the caves (Forbes & Bestland, 2007). There are three main sediment types within the caves which entered via minor runoff flows; brown organic-rich sandy silts, reddish sandy silts and homogenous yellowish sands (Forbes & Bestland, 2007).

Blanche Cave was discovered by European settlers in 1845 CE (Darrénougué et al., 2009). It consists of three main chambers with debris and sediment cones that lie under large roof collapse windows in each chamber (Figure 2b) (St. St Pierre et al., 2012). The

collapse of part of the roof occurred during the late Quaternary in order to accumulate Pleistocene aged sediments and fossils (Darrénougué et al., 2009). The sediments within the cave are characteristically well stratified and deep (Darrénougué et al., 2009), containing laminations that lie within broader sedimentary units (Macken et al., 2013). These layers contain a predominantly owl pellet derived fossil record (Macken & Reed, 2013), in addition to phosphate minerals of whitlockite and apatite that are the result of in situ reactions of decomposing bat guano and fine grained clastic minerals (Forbes & Bestland, 2007). Blanche Cave has a designated Australian Speleological Federation Number, 5U6. The 5 represents the state of South Australia, U refers to the upper south-east, and the number 6 is assigned from the closest entrance window of the cave (Macken et al., 2013). The excavation site contains a high density of bone material within the stratified layers (Figure 3), which fall across major changes in climate. These characteristics allow for the analysis of faunal response to fluctuation of palaeoclimate, such as glacial cycles and the structure of small mammalian communities (Macken & Reed, 2014). The climate in the south-eastern area of South Australia is temperate with mild, long, dry summers and cool, wet winters. The annual rain fall of Naracoorte is approximately 580 mm, with a mean maximum temperature of approximately 21°C (Macken & Reed, 2014).

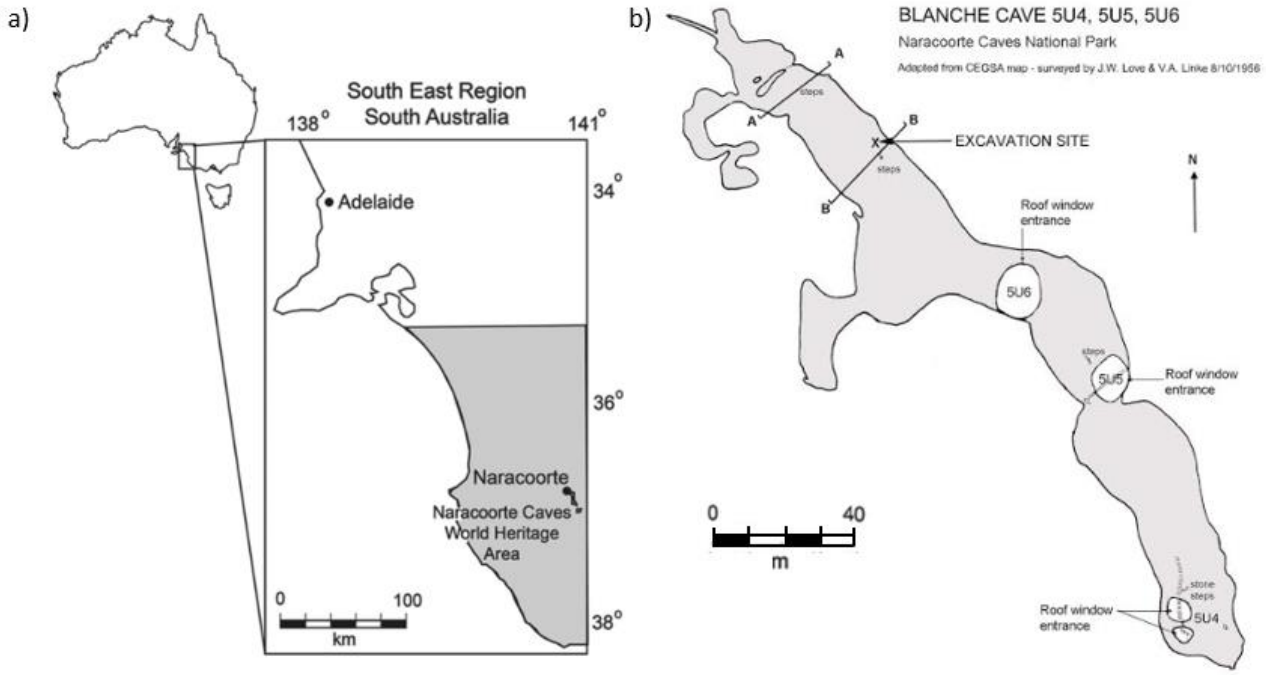

Figure 2: a) Location of the Naracoorte Cave World Heritage Area (NCWHA), South-eastern South Australia. Map adapted from Macken, & Reed, (2013). b) Cave map of Blanche Cave with the excavation site from which the sample of this study were previously obtained. Map supplied by E. Reed.

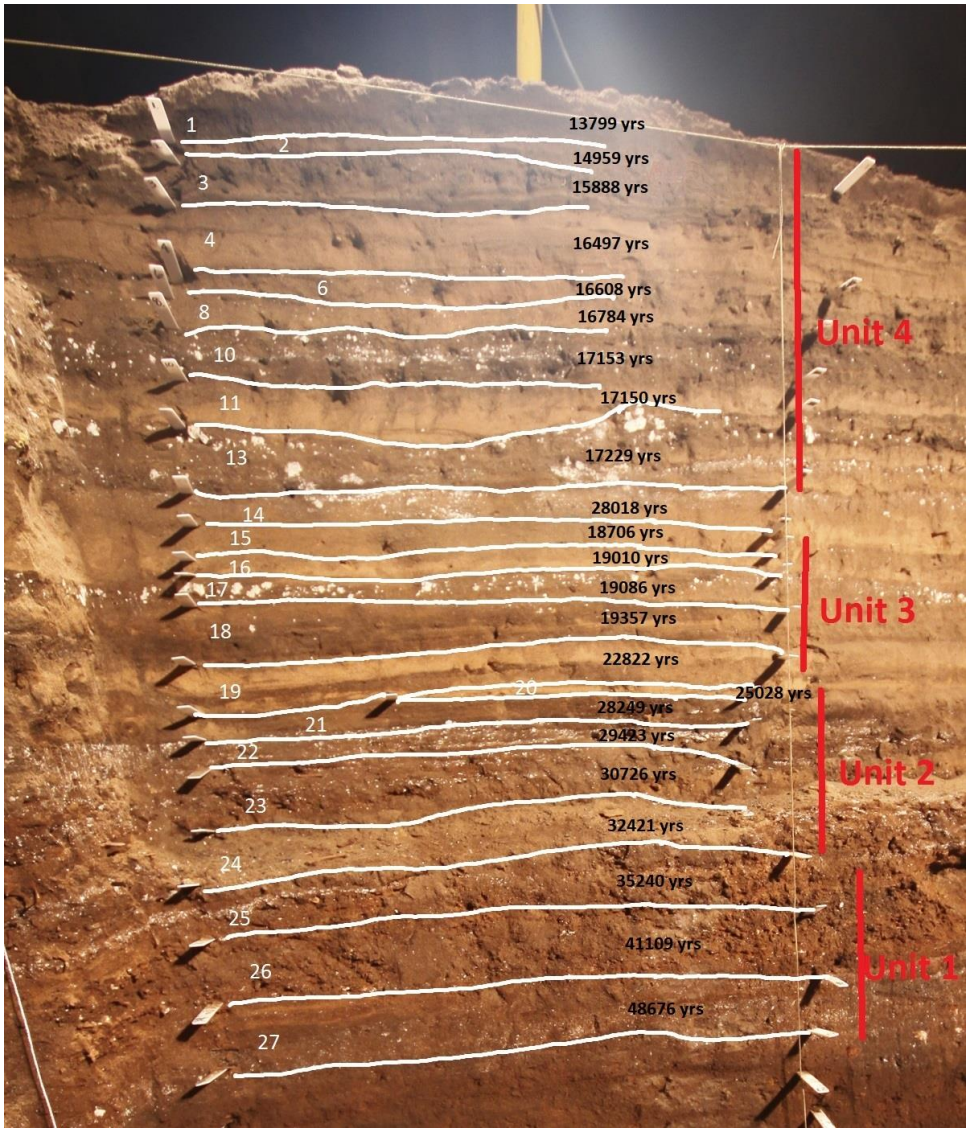

Figure 3: Stratigraphic sequence of the first 27 layers of Blanche Cave excavation site, Naracoorte Caves World Heritage Area (NCWHA). Depth is approximately the first metre below cave ground surface. Mean ages for each layer obtained from Macken et al. (2013). The layers are divided into climatic-stratigraphic units; unit 1 – pre-glaciation (layers 27-25), unit 2 – early glaciation (layers 24-20), unit 3 – Last Glacial Maximum (layers 15-19) and unit 4 – deglaciation (layers 13-1). Photo taken by Steve Bourne.

Background

The analysis of stable isotopes has been a great advancement in the field of palaeontology, enabling reconstruction of diet and environmental conditions from fossil remains. This has given insight into behaviours and habitats of extinct species, as well as the past behaviours of extant communities (Clementz, 2012). Stable isotope analysis of mammalian bioapatite derived from teeth has become an established proxy for constructing environmental and dietary conditions of mammalian communities (Gehler et al., 2012). Bioapatite studies have predominantly concentrated on large to medium sized mammals, due to the relatively smaller proportion of material required for analysis (Barham et al., 2017). Some of these studies include dietary reconstruction of Late Pleistocene cave bears in Romania (Robu et al., 2017) and Yellowstone (Robu et al., 2013), along with 4-1 ma fossilised large herbivore remains from the Turkana Basin, Kenya (Cerling et al., 2015). In Australia, previous studies have also focused on larger mammals. Studies in stable isotopes of present day kangaroos in Southern Australia (Brookman & Ambrose, 2012) and across a latitude gradient (Brookman & Ambrose, 2013), have been conducted to determine the reliability of palaeoclimate reconstructions. Isotope analysis of fossil remains to reconstruct climate and habitat conditions in the Pliocene in south-eastern Queensland have also focused on kangaroos and other large mammals including two megafauna, *Protemnodon* sp. indet and *Euryzygoma dunense* (Montanari et al., 2013). Studies on small mammal bioapatite are comparatively rare to that of large mammals, and consequently, small mammalian fossils have been overlooked despite life characteristics that make them a favourable candidate for recording local climate (Gehler et al., 2012). These characteristics include their ability to inhabit numerous ecosystems of varying sizes (Gehler et al., 2012), large

populations and their short life span (Gehler et al., 2012), which provide a higher temporal scale of change (Barham et al., 2017).

Rodents are found in the fossil record from the Palaeogene onwards, with the Cenozoic having a widespread fossil record in terrestrial deposits. They are often seen in high abundances due to predation of ancient avian predators which form the most common accumulation sites (Gehler et al., 2012). As they have constantly growing incisors, the isotopic signatures analysed represent approximately four to twelve weeks prior to the death of the individual (Gehler et al., 2012).

The carbon isotopic composition of rodent teeth is commonly assumed to represent consumed vegetation, which in turn can be used to infer vegetation coverage, palaeovegetation, resource partitioning and dietary strategies between species (Gehler et al., 2012). Plants use three different photosynthetic pathways; C_3 (Calvin-Benson), C_4 (Hatch-Slack) and CAM (Crassulacean Acid Metabolism). Most plants either use a C_3 or C_4 pathway, which have distinctive $\delta^{13}C$ values due to a difference in the fractionation of atmospheric carbon (Johnson et al., 1997). C_3 plants make up approximately 95 % of plants on earth and mainly consist of high altitude and latitude, temperate, shade tolerant plants (Brookman & Ambrose, 2013). This includes most shrubs and all woody trees (Gehler et al., 2012). These plants exhibit a larger discrimination against heavy carbon isotopes (^{13}C) (Quinn, 2010), which consequently gives C_3 plants a lower $\delta^{13}C$ value, between -36 ‰ and -22 ‰ (Gehler et al., 2012), with an average of -26.3 ± 2.1 ‰ for the Lake Eyre area (Miller et al., 2005). C_4 plants discriminate against the heavier carbon isotopes to a lesser extent and have a greater efficiency in the conversion of CO_2 into carbohydrates. These plants are better adapted to low water availability, and their C_4 mechanism means they can close stomata during

the day, thus losing less water to evapotranspiration. C_4 photosynthesis is found in only 3 % of vascular plant species, but these species are abundant, making up ~25 % of plant photosynthesis (Edwards et al., 2010). C_4 plants consist of most grasses and shrubs that have adapted to these conditions (e.g. saltbush) and are commonly found in high temperature, arid environments with strong sunlight or strongly seasonal climates (Brookman & Ambrose, 2013). The $\delta^{13}C$ values of these plants are higher and have a range of -15 to -10 ‰ (Gehler et al., 2012), and an average of -13.7 ± 0.7 ‰ in the Lake Eyre area (Miller et al., 2005). CAM make up approximately 4 % of all plants on earth, which consist of mainly succulents. CAM plants switch between C_3 and C_4 cycles which give them a varying $\delta^{13}C$ value (Gehler et al., 2012). C_4 plants have represented a major component of the Australian biomass since the late Pliocene (Andrae et al., 2018).

The oxygen isotopic component of the bioapatite is derived from the metabolic water of the individuals, which is obtained from ingested water (Johnson et al., 1997). For mammals that have a compulsive behaviour to drink water, the sources in which they obtain their water can vary in isotopic composition due to changes in meteorological and hydrological processes (Montanari et al., 2013). These sources can be a combination of surface water types (e.g. streams, lakes, ponds, etc.), each having different $\delta^{18}O$ values to precipitation (Montanari et al., 2013). For individuals without a compulsive behaviour to drink, like some small mammals, including one of the extant species, *Pseudomys australis* (Brandle & Pavey, 2008), they obtain their water from their diet, such as leaf water. Leaf water is isotopically enriched which gives a higher $\delta^{18}O$ value, which reflects relative humidity due to evapotranspiration (Montanari et al., 2013). Mammalian bioapatite contains both phosphate ($\delta^{18}O_{PO4}$) and carbonate

($\delta^{18}O_{CO3}$) bound oxygen (Gehler et al., 2012), both of which can be analysed to infer past environmental change. Of the two, phosphate bound oxygen is considered to be more robust and resistant to post-depositional alteration (Iacumin et al., 1996).

METHODS

The samples in this study were obtained from the first 27 layers in the Blanche Cave excavation site (Figure 2b and Figure 3), which is approximately 1 m in depth, spanning over an age range of approximately 49 – 14 ka. Layer 14 was excluded from this study as it has been reworked (Darrénougué et al., 2009; Macken et al., 2013). Samples were only taken from layers that had five or more incisors still within an identifiable lower jaw (dentary). The dentaries that were chosen had no visible digestive etching or post-depositional alterations to ensure that there was no extra contaminants that would affect the analysis. The total collection for analysis was 401 individual teeth, with between five and fifteen teeth extracted from identified dentaries of the three species of *Pseudomys (Pseudomys auritus, P. australis* and *P. shortridgei*), with an average of 10 teeth per sample. The relative abundance of each species was calculated using the number of specimens (NISP) for each layer and the four climatic-stratigraphic units.

$$Relative\ Abundance\ (\%) = \frac{NISP_x}{NISP_{total}} \times 100$$

Where $NISP_X$ corresponds to the number of individual specimens of one species per measured unit, and $NISP_{total}$ corresponds to the total number of individual specimens per measured unit (Macken et al., 2012). NISP was chosen over minimum number of individuals (MNI), even though NISP gives non-independent values, as a single animal may contribute multiple diagnostic elements (both right and left dentary). However,

there is a strong linear correlation between MNI and NISP, R^2= 0.99 in small mammals, and therefore they are proportionally related (Macken et al., 2012).

The teeth were crushed to a fine powder using an agate mortar and pestle. Methanol was used to wipe out the mortar and pestle to remove contaminants between samples. The pre-treatment, outlined by Kohn et al (1997) was conducted to remove any organic matter as well as surface carbonates. Approximately 20 mg of crushed sample was soaked in 30 % hydrogen peroxide for 24 hours and rinsed five times with reverse osmosis water (RO water). After rinsing, the sample were then soaked for an additional 24 hours in 1 M calcium acetate buffer solution, rinsed another five times with RO water and dried at 50ºC for approximately 24 hours or until the powder was dry.

For analysis of oxygen and carbon isotopes in carbonate, approximately 2 mg of pre-treated sample powder was reacted with 100 % phosphoric acid for 15 minutes (Gehler et al., 2012) using a Gas Bench device coupled via continuous flow with a Nu Horizon Isotope Ratio Mass Spectrometer (IRMS). The raw data obtained was normalised to P3, UAC and CO8. The data was reported in δ-notation in per mil (‰), which was relative to the international isotope reference standards. For the oxygen data ($\delta^{18}O$) the reference standard is Vienna Standard Mean Ocean Water (VSMOW), and for the carbon data ($\delta^{13}C$) Vienna Pee Dee Belemnite (VPDB) was used (Johnson et al., 1997).

$$\delta^{18}O \text{ or } \delta^{13}C\ (‰) = [\left(\frac{R_{sample}}{R_{standard}}\right) - 1] \times 100$$

Where R_{sample} and $R_{standard}$ are the ratios of the light and heavy isotopes, carbon ($^{13}C/^{12}C$) and oxygen ($^{18}O/^{16}O$), for both sample and standard.

Mammalian bioapatite has a carbon isotopic enrichment factor between 9 to 15 ‰ compared to diet (Gehler et al., 2012). The average of this enrichment, approximately 12 ‰, was used to obtain $\delta^{13}C_{diet}$ (Brookman & Ambrose, 2013).

$$\delta^{13}C_{diet} = \delta^{13}C_{sample} - \delta^{13}C_{enrichment}$$

The analysis of the phosphate bonded oxygen was achieved using the method outlined by Trayler and Kohn (2017). Approximately 1 mg of pre-treated sample was reacted in 0.5 M nitric acid until the sample had completely dissolved, this took approximately 12 hours. Once sample had fully dissolved, 0.5 M of potassium hydroxide was added to neutralise the solution. Potassium fluorite (0.36 M) was then added to precipitate out calcium in the form of calcium fluoride. Following mineral precipitation, the supernatant was decanted and placed into a clean centrifuge tube. Silver amine solution (0.5 M ammonium nitrate, 0.2 M silver nitrate and 0.74 M ammonium hydroxide) was added and then placed in an oven at 30ºC overnight to allow the ammonia to exsolve gradually. Silver phosphate was the resulting precipitate, which was rinsed five times with RO water and placed back into the 30ºC oven overnight. Approximately 0.5 mg of powder was weighed into a silver cup and was analysed by temperature conversion isotope ratio mass spectrometry using an Elemantar high temperature pyrolysis furnace coupled via continuous flow to a Nu Horizon Mass Spectrometer. The raw data obtained was normalised to keratin (Kudu Horn (KHS), and Caribou Hoof (CBS)), IAEA-NO-3, NBS-127 and USGA-32, and reported in δ-notation in per mil (‰).

RESULTS

Sedimentation Chronology

The samples analysed from Blanche Cave have an age range of ~ 49 to 14 ka (Macken et al., 2013). The layers from which the samples were obtained have been grouped into climatic-stratigraphic units; pre-glaciation (layers 27-25, ~ 49 – 35 ka), early-glaciation (layers 24-20, ~ 32 – 25 ka), Last Glacial Maximum (layers 19-15, ~ 22 -19 ka) and the deglaciation (layers 13-1, ~ 17 to 14 ka). These ages have been obtained from Macken et al. (2013), and for simplicity, all figures have a mean age for each layer.

Relative Abundance of Fossil Teeth

The relative abundances of the three species of *Pseudomys* varied throughout the layers (Figure 4). *P. shortridgei* was found to have a comparatively stable relative abundance, which ranged between 10.4 % and 50 %, with an average of 24.7 %. This species showed an increase in variability between layer 21 and 13 and was the most abundant species in layer 21 (Figure 4). The relative abundance that was seen between *P. australis* and *P. auritus* had values between 11.9 to 65.7 % and 12.5 to 69.9 %, and averages of 36.6 % and 38.7%, respectively. *P. auritus* was the most abundant in most layers, with a declining trend from layers 22 to 14. *P. australis* was the most abundant species in layers 23, 19 to 13 and 3 (Figure 4).

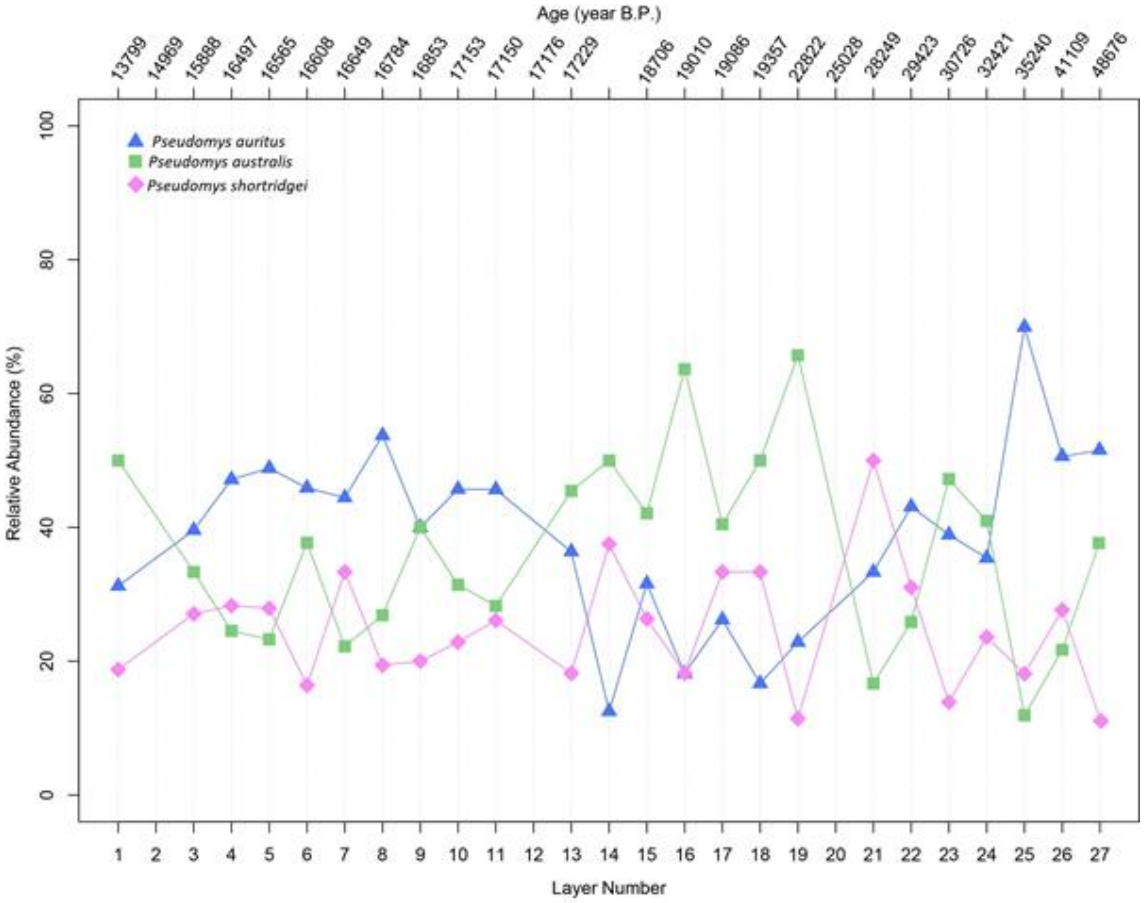

Figure 4: Plot of the relative abundance (%), determined by the number of specimens (NISP) from fossilised lower jaws (dentaries), obtained from the Blanche Cave excavation site. The three species of *Pseudomys* (*P auritus, P. australis* and *P. shortridgei*) were plotted against the stratigraphic layers in the Blanche Cave excavation site and the age in years before present (years B. P.). The age for layer 14 has been excluded from the above figure as this layer has been reworked. Mean ages obtained from Macken et al. (2013).

The relative abundances of the species over the climatic-stratigraphic units showed that *P. shortridgei* had no change in the relative abundance over all the climatic-stratigraphic units (Figure 5), which had values that ranged between 23.6 % and 24.3 %, with an average of 24.0 %. Between *P. australis* and *P. auritus*, their relative abundances fluctuated across climatic-stratigraphic units, with values between 19.7 to 51.3 % and 24.8 to 56.1 %, with averages of 35.2 % and 40.9 %, respectively. In units 1 and 4, *P. auritus* was the most abundant, with *P. australis* being the most abundant species in unit

3. The relative abundance between these two species in unit 2 are comparatively the same (Figure 5).

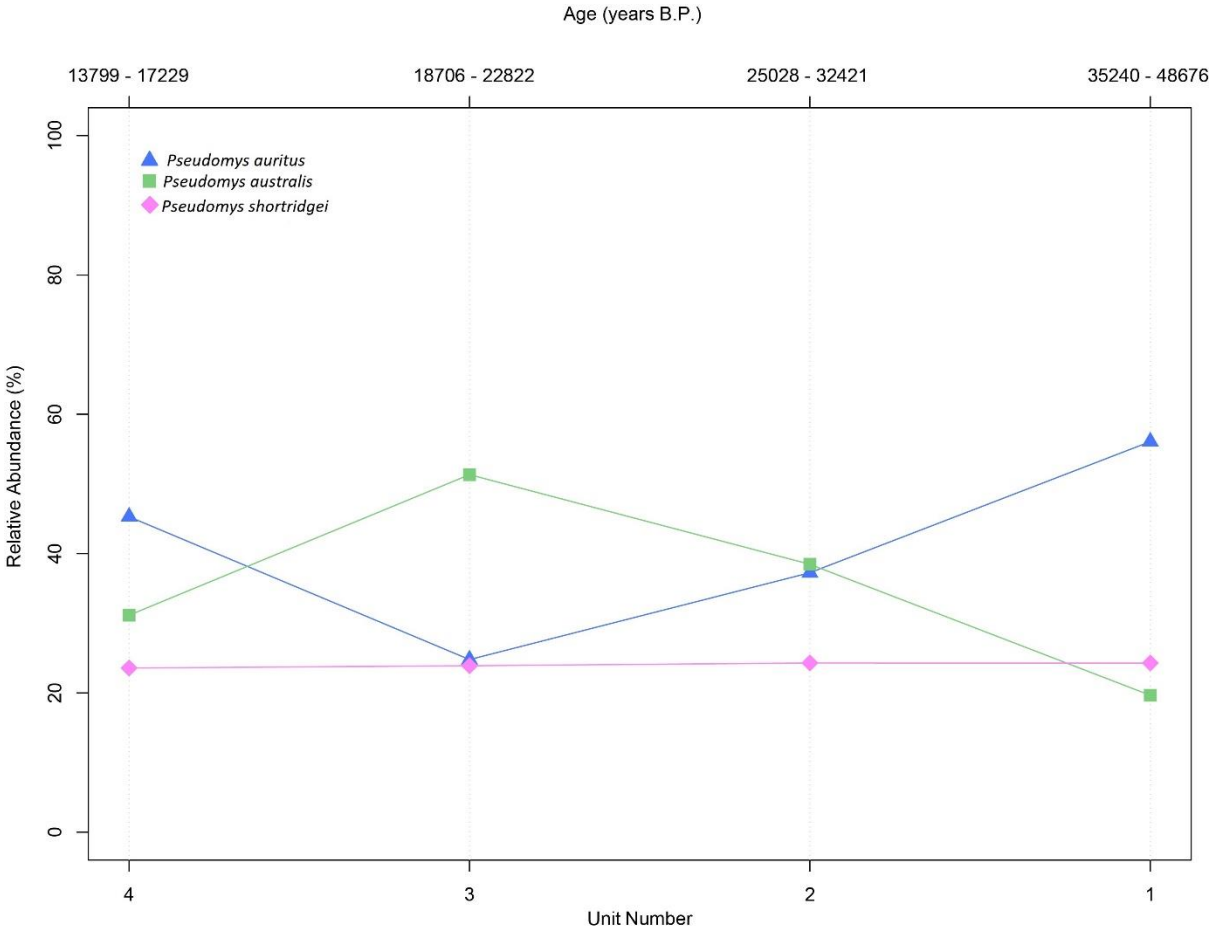

Figure 5: Relative abundance (%), determined from the number of specimens (NISP) of fossilised dentaries from Blanche Cave for three species of *Pseudomys* (*P. auritus, P. australis* and *P. shortridgei),* plotted against the climatic-stratigraphic units; unit 1 – pre-glaciation (layers 27-25), unit 2 – early glaciation (layers 24-20), unit 3 – Last Glacial Maximum (layers 19-15) and unit 4 – deglaciation (layers 13-1), and age in years before present (years B. P.). Mean ages obtained from Macken et al. (2013).

Carbonate Isotope Variability

Both $\delta^{18}O_{CO3}$ and $\delta^{13}C$ were analysed from the carbonate component of the bioapatite. The $\delta^{13}C$ over the three species varied between layers (Figure 6a). The $\delta^{13}C$ values for the teeth of *Pseudomys shortridgei* ranged between -6.6 and -10.7 ‰ with an average of -8.9 ‰. These values were relatively higher compared to *P. auritus* and *P. australis*, which had similar ranges of -7.5 to -11.5 ‰ and -8.2 to -11.9 ‰, and averages of -9.9

‰ and -10.2 ‰, respectively, with a strong correlation of $R^2 = 0.75$. Correlations with *P. shortridgei* were not reported as there were not enough data points to obtain an accurate correlation. The estimated $\delta^{13}C$ values for diet for *P. shortridgei* ranged between -18.6 and -22.7 ‰, with an average of -20.9 ‰. *P. auritus* and *P. australis* had estimated diet $\delta^{13}C$ values between -19.5 to -23.5 ‰ and -20.2 to -23.9 ‰, with averages of -21.9 ‰ and -22.2 ‰, respectively. Throughout the layers, all three species exhibited a relative increase in $\delta^{13}C$ from layers 27 to 22, followed by a decrease in layers 19 to 15. *P. australis* and *P. auritus* showed an increase in $\delta^{13}C$ from layer 13, with the overlying layers displaying no apparent trend (Figure 6a). From layer 17 to 10, *P. shortridgei* displayed an increase followed by a decrease to layer 3 (Figure 6a).

The $\delta^{18}O_{CO3}$ values ranged between species. *P. auritus* $\delta^{18}O_{CO3}$ fell between -1.4 and 1.9 ‰, with an average of 0.2 ‰, *P. australis* values ranged from -4.9 to 1.2 ‰, with an average of 0.2 ‰, and the values of *P. shortridgei* ranged between -1.8 and -0.3 ‰, with an average of -0.9 ‰. The $\delta^{18}O_{CO3}$ values of *P. shortridgei* were consistently lower than the other two species except for layer 9, where *P. australis* had the lowest value (Figure 6b). The correlation between *P. auritus* and *P. australis* was weak, with $R^2 = 0.36$. The trends seen in Figure 6b were relatively stable across all species, with *P. shortridgei* having no trend, where *P. auritus* and *P. australis* show more variability.

Phosphate $\delta^{18}O$ Variability

The phosphate bound $\delta^{18}O_{PO4}$ analysed from the bioapatite of *P. auritus* had the largest range between values of 21.3 to 24.2 ‰, with an average of 22.7 ‰. The range in $\delta^{18}O_{PO4}$ for *P. australis* and *P. shortridgei* was 21.1 to 23.1 ‰ and 21.9 to 23.5 ‰, with averages of 22.4 ‰ and 22.5 ‰, respectively. The R^2 value between the $\delta^{18}O_{PO4}$ of *P.*

australis and *P. auritus* showed no correlation (R^2=-0.085) when the entire dataset was considered. The general trend of the species throughout the layers showed that there was a relative increase from layer 27 to 19, followed by a relative decrease from layer 19 to 3 (Figure 6c). Between *P. australis* and *P. auritus*, the fluctuating trends were inversely proportional from layer 27 to 15 and 4 to 3; whereas layers 13 to 5 showed a proportional relationship (Figure 6c).

The average offset between the phosphate and carbonate bound oxygen in the bioapatite over the three species of *Pseudomys* was 8.2 ‰. For *P. auritus* the average offset between $\delta^{18}O_{PO4}$ and $\delta^{18}O_{CO3}$ was 8.4 ‰ with a range of values between 6.9 and 9.3 ‰. *P. australis* had an offset range of 2.7 to 9.7 ‰ and an average of 8.7 ‰. The average offset between the two $\delta^{18}O$ values was 7.6 ‰ in *P. shortridgei*, with a range of 6.9 to 8.3 ‰.

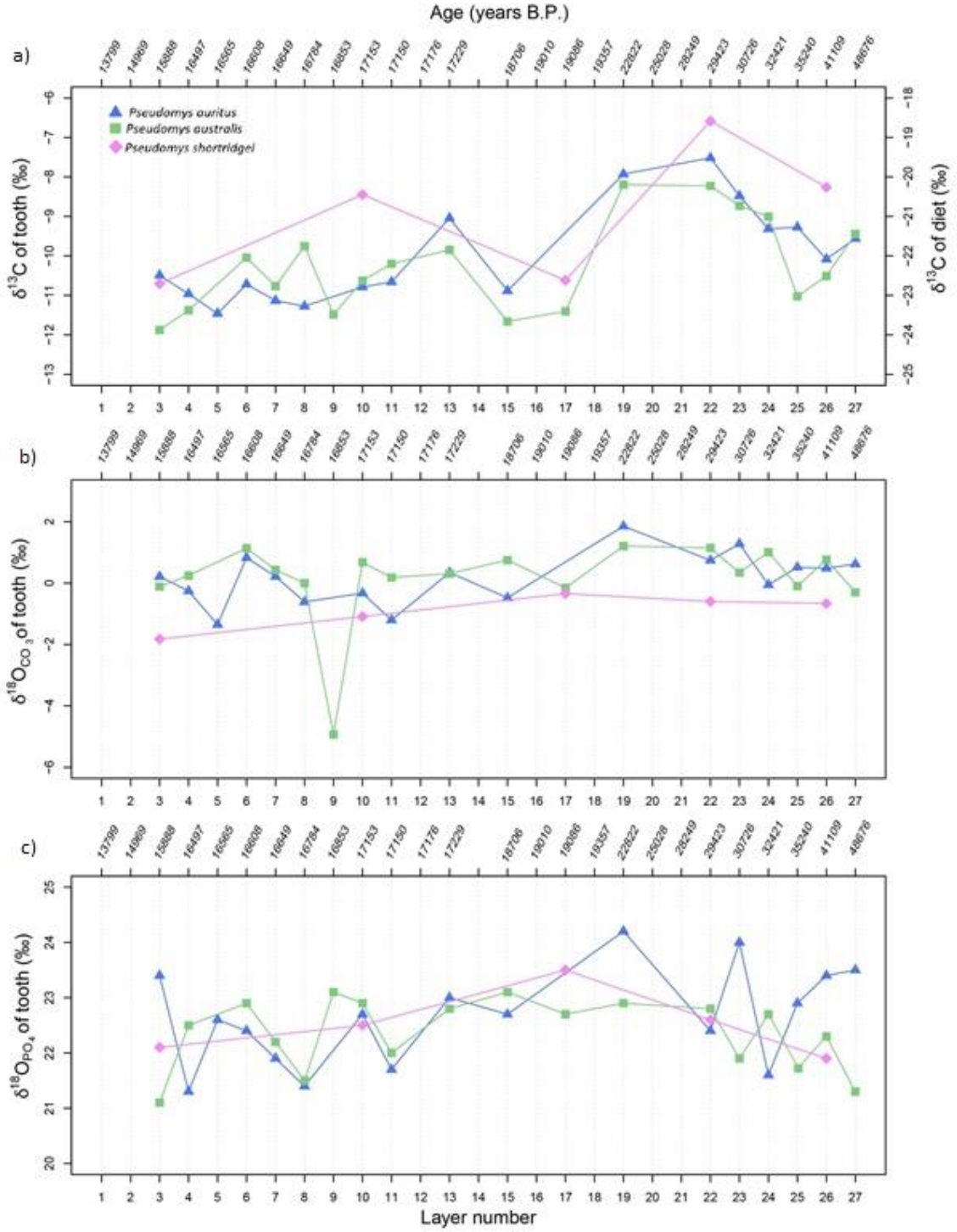

Figure 6: Plots of stable isotope data from fossilised incisors of three species of *Pseudomys* (*P auritus, P. australis* and *P. shortridgei*) analysed by an Isotope Ratio Mass Spectrometer (IRMS), over stratigraphic layers in the Blanche Cave excavation site, and age in years before present (years B. P.). The age for layer 14 has been excluded from the above figure as this layer has been reworked. Mean ages obtained from Macken et al. (2013). a) $\delta^{13}C$ values in percent per mil (‰) of both tooth and diet signatures for the three *Pseudomys* species. b) $\delta^{18}O_{CO3}$ values (‰) of the carbonate bound oxygen from the tooth of the three *Pseudomys* species. c) $\delta^{18}O_{PO4}$ values (‰) of the phosphate bound oxygen from the tooth of the three *Pseudomys* species.

$\delta^{13}C$ vs $\delta^{18}O_{PO4}$

In unit 1, it was seen that there were relatively low $\delta^{13}C$ values with a wide range of $\delta^{18}O$ values (Figure 7). Unit 2 displayed high $\delta^{13}C$ values with once again a varying range of $\delta^{18}O$ values. Low $\delta^{13}C$ values with high $\delta^{18}O$ were seen in Unit 3 with some of the values displaying higher $\delta^{13}C$. Unit 4 displayed low $\delta^{13}C$ and predominantly low $\delta^{18}O$ (Figure 7). There were no clear patterns observed in any of the species within any of the units.

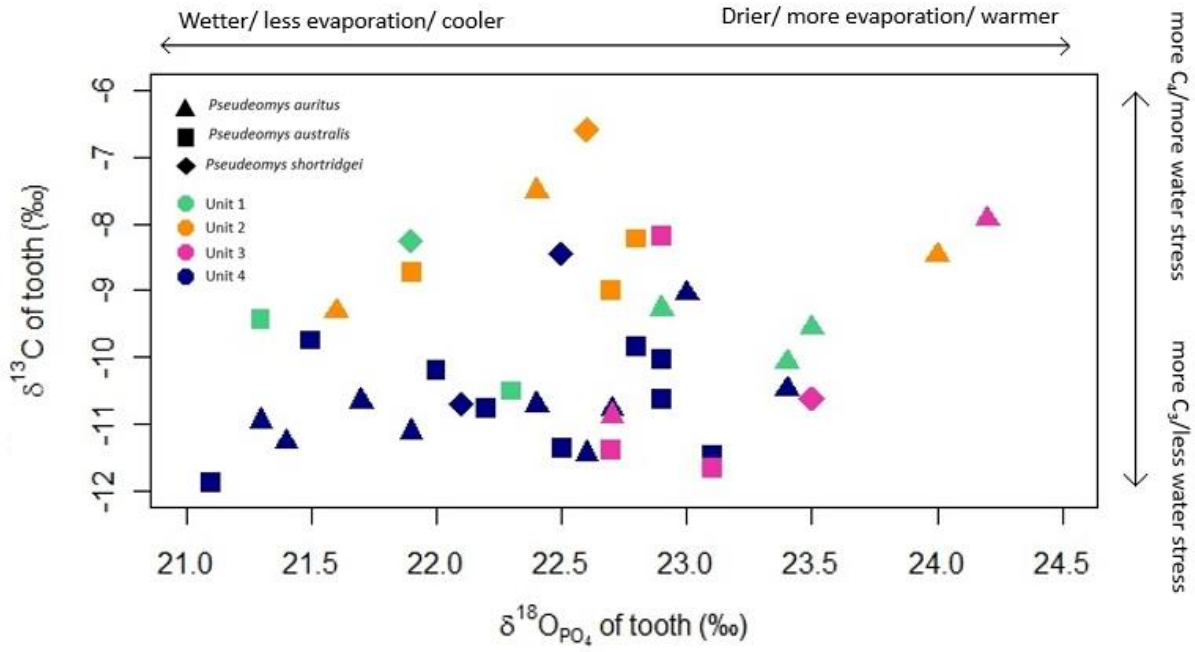

Figure 7: Plot of $\delta^{13}C$ (‰) against $\delta^{18}O_{PO4}$ (‰) for the three *Pseudomys* species (*P. auritus, P. australis* and *P. shortridgei*). The points displayed are the data obtained from each species over the 27 layers of Blanche Cave Excavation Site, Naracoorte Caves World Heritage Area. The layers have been colour coded into climatic-stratigraphic units; unit 1 – pre-glaciation (layers 27-25), unit 2 – early glaciation (layers 24-20), unit 3 – Last Glacial Maximum (layers 19-15) and unit 4 – deglaciation (layers 13-1).

DISCUSSION

Stable isotope analyses provide valuable context to aid the interpretation of fossil deposits and their ecological drivers. Such data are also commonly used tracers of climatic change. At Blanche Cave, the carbon and oxygen isotope data from rodent teeth indicated a notable shift in the climate and environment leading into and out of the Last Glacial Maximum (between 50-10 ka)

Isotopic Interpretations

The $\delta^{13}C$ can be interpreted as two main effects on the vegetation/climate. Firstly is the change in the dominant photosynthesis pathway used by the plants in the area (C_3 vs C_4), and the second is the water availability for the plants (C_3 plants that have experienced water stress will display a higher $\delta^{13}C$ value). However, these two mechanisms reinforce the same interpretation, an increase in $\delta^{13}C$. When it's dry there is a shift towards a dominance in C_4 plants, as well as an increase in the $\delta^{13}C$ values of C_3 plants.

$\delta^{13}C$ values showed a decreasing trend over climatic-stratigraphic unit 1 (layers 27-25), pre-glaciation. This suggested that the vegetation consumed by the rodents moved towards a more C_3 dominated environment, indicating a more closed landscape. The climatic-stratigraphic unit 2 (layers 24-20), early-glaciation, showed an increasing trend in $\delta^{13}C$, which suggested that there was a shift from more C_3 to more C_4 dominance and the opening of the landscape. This also suggested more water stressed C_3 plants. A decreasing trend in $\delta^{13}C$ values was seen in climatic-stratigraphic unit 3 (layers 19-15), LGM, which implied that there was a shift from the C_4 dominated environment seen in

unit 2, to a C_3 dominated environment. The overlying layers that make up climatic-stratigraphic unit 4 (layer 13 -1), deglaciation, had more stable $\delta^{13}C$ values that indicated C_3 vegetation dominance and suggested that there is a more closed environment compared to unit 3. Interestingly, the $\delta^{13}C$ of *P. shortridgei* contrasted with the values for *P. auritus* and *P. australis*, whereby the *P. shortridgei* $\delta^{13}C$ values were consistently higher. Several reasons for this pattern were viable, including a slight preference by *P. shortridgei* for C_4 vegetation. However, higher $\delta^{13}C$ values were also observed in seed carbon relative to leaf matter (Cernusak et al., 2009) and it was feasible that this explained the difference in $\delta^{13}C$ between *P. shortridgei* teeth and those from the other rodents analysed. The $\delta^{13}C$ values between *P. australis* and *P. auritus* showed a relatively similar trend which suggested that they ate similar vegetation.

The $\delta^{18}O$ can be interpreted as the leaf water that was ingested by the individuals or local source water. Leaf water is isotopically enriched compared to surface water, however, an increase in $\delta^{18}O$ would be seen as an effect of high evaporation and low precipitation, indicating a drier and possibly warmer environment.

There are two oxygen bound pathways in bioapatite, carbonate ($\delta^{18}O_{CO3}$) and phosphate ($\delta^{18}O_{PO4}$). From the results it was seen that the $\delta^{18}O_{CO3}$ and $\delta^{18}O_{PO4}$ displayed similar trends, however, when comparing the values it was clear that the $\delta^{18}O_{PO4}$ recorded signatures that showed more detail. As the phosphate bound oxygen pathway is more resistant to post-depositional alterations (Barham et al., 2017), the signatures obtained from the phosphate bound $\delta^{18}O$ was of greater focus.

The carbonate bound $\delta^{18}O$ showed that through unit 1 and 2, there was a slight increase in $\delta^{18}O$ values. This suggested a lower effective moisture at this time or drier conditions. Through units 3 and 4 there was a steady declining trend, which indicated

the transition into higher effective moisture conditions or the availability of more water. *P. shortridgei* showed a steady declining trend over all four units, whereas *P. australis* and *P. auritus* displayed similar trends. However, in layer 9 which falls within unit 4, there was a rapid decrease in $\delta^{18}O$ for *P. australis*. As there was no other data collected from the other species in this layer, this signature cannot be regarded as an outlier. Excluding layer 9, the variation between the $\delta^{18}O$ values between species was very small, therefore implying that water was obtained from similar sources by all taxa.
An increase in inter-layer variability throughout the four units was seen in the phosphate bound $\delta^{18}O$ in comparison to the carbonate bound $\delta^{18}O$. The same general trend of an increase in $\delta^{18}O$ through unit 1 and 2 was interpreted as lower effective moisture or drier conditions. Through unit 3, there was a decrease in $\delta^{18}O$ values which suggested an increase in effective moisture or wetter conditions. This trend was continued through unit 4, however, there was more fluctuation between values which was interpreted as a fluctuation of wetter drier cycles. From units 1, 2 and 3, an inverse relationship was observed between *P. auritus* and *P. australis*, which suggested that they would have obtained their water source from different places. However, in unit 4, this relationship became proportional, which indicated they get their water from similar sources in this unit.

Climatic Reconstruction

Using the stable isotopic data above and published climatic records, a reconstruction of the climate in south-east Australia was constructed over the last glacial cycle. As *P. shortridgei* had so few data points in this study, the main focus of climate predictions was on *P. auritus* and *P. australis.*

From previous climatic records, it was seen that pre-glaciation (~49-35 ka) climate was warmer than that of the LGM (Meerbeeck et al., 2009), however, the annual temperature was 6°C lower than today (Williams et al., 2006). Lopes dos Santos et al. (2013) suggested that the highest percentage of C_4 plants was seen between 58-44 ka. This was followed by an increase in C_3 eucalyptus woodland around 39-30 ka (Dodson, 1977). These records coincided with the vegetation interpretations of dominance in C_3, with warm and drier conditions seen in *P. auritus* and *P. australis* during pre-glaciation.

Early glaciation (~32-25 ka) was characterised by cooling around 32 ka (Reeves et al., 2013). There was an increase in dust transport at this time, which was most likely caused by an increase in aridity seen in the Murray Darling Basin (Lopes dos Santos et al., 2012). This was interpreted as drier and cooler conditions (Reeves et al., 2013). An increase in sediment deposition in Robertson Cave, from the NCWHA, supported cooler, drier conditions in this period (Petherick et al., 2013). Changes in vegetation mirrored this interpretation, where grass and herb taxa (C_4) were dominant at the expense of arboreal taxa (C_3) (Williams et al., 2006), implying the presence of open woodlands and herblands. Speleothem records from NCWHA showed a positive effective moisture through the early glaciation (Macken & Reed, 2014). This was supported by high fluvial activity in the southern part of the Murray Darling Basin, which coincided with the first appearance of glaciers in the Snowy Mountains and therefore could be due to seasonal snow runoff (Petherick et al., 2013). The vegetation reconstruction from these studies agreed with the $\delta^{13}C$ obtained from the bioapatite. From the $\delta^{18}O$ and the $\delta^{13}C$ of this study, it was inferred that the climate at this time

exhibited cooler, drier conditions which was seen by the lower effective moisture levels (higher $\delta^{18}O$) and dominance of C_4 vegetation at this time (higher $\delta^{13}C$).

The LGM (~22-19 ka) had the lowest temperature of approximately 10°C below present (Lopes dos Santos et al., 2012). There was also a decrease of sea surface temperature at this time, of about 5-7°C (Turney et al., 2006). Eustatic sea level ranged from 60-120 m below modern day sea level, which caused Naracoorte to be further from the ocean and consequently drier (Petherick et al., 2013). Falster et al. (2018) reported a decrease in effective moisture from 24-19 ka, this implied that the LGM was a relatively dry period. This was supported by an increase in the organic biomarker levoglucosan in the sediments of the Murray Canyons, South Australia, which was interpreted as an increase in wildfire occurrence (Lopes dos Santos et al., 2013). The vegetation assemblage for this time showed a dominance of herbaceous, semi-arid shrublands which implied dry conditions (Builth et al., 2008; Dodson, 1977; Falster et al., 2018; Petherick et al., 2013; Reeves et al., 2013). However, at the height of the LGM, there was a high concentration of eucalypt and casuarinaceae pollen (Builth et al., 2008; Williams et al., 2006). This appearance of C_3 plants at the height of the LGM suggested an increase of effective precipitation (Falster et al., 2018). This increase was also seen in the speleothem records from Naracoorte Caves, South Australia (Reeves et al., 2013). This implied that there were humid periods in a mostly arid dominated environment. However, the LGM was generally characterised by cool and drier conditions (Falster et al., 2018). This change from C_4 dominance to C_3 dominance in the LGM was reflected in the vegetation reconstruction from the bioapatite of the three *Pseudomys* species. The $\delta^{18}O$ values showed that there was a slight increase in water availability and/or an

increase in effective moisture as discussed by Falster et al. (2018), but was generally drier.

The first evidence for the deglaciation period occurred around 20-19 ka (Pedro et al., 2011; Reeves et al., 2013), with a warming of 10°C due to an increase of sea surface temperature off the east coast of Australia and global sea level rise (Falster et al., 2018; Lopes dos Santos et al., 2012; Petherick et al., 2013; Reeves et al., 2013). This rise in sea level led to a decrease in aridity and moisture stress on plants (Falster et al., 2018). The warming that is associated with the deglaciation has been reflected in the pollen records, showing a gradual increase in arboreal taxa such as eucalypts and casuarinaceae with a decrease in herbaceous vegetation, which indicated a closed landscape (Falster et al., 2018; Petherick et al., 2013; Reeves et al., 2013; Turney et al., 2006). At approximately 15 ka, there was a shift to drier conditions with an increase in chenopodiaceae and asteraceae, C_4 vegetation (Falster et al., 2018; Petherick et al., 2013; Turney et al., 2006). Falster et al. (2018) concluded that after this time, $\delta^{13}C$ became more stable. The vegetation reconstruction of this study showed an increase of herbaceous vegetation (C_4) at the beginning of deglaciation, followed by more stable $\delta^{13}C$ values, which suggested a C_3 dominance. The $\delta^{18}O$ showed a wetter environment after the LGM with the phosphate bound $\delta^{18}O$ showing drier periods when the $\delta^{13}C$ values are stable.

Species Response to Climate

Mammal communities in the Naracoorte Caves World Heritage Area have been stable for thousands of years including the last glacial cycle (Macken & Reed, 2014). The relative abundances of the three species of *Pseudomys* have varied over the first 27

layers of Blanche Cave, South Australia. Over the layers, *P. auritus* was the most abundant compared with *P. australis* and *P. shortridgei,* the only exceptions to this was from layers 15-20, the LGM, where *P. australis* was the most abundant. *P. shortridgei* was commonly the least abundant throughout all the units; however, it was the most abundant in layer 21 which falls in the early glaciation period. When looking at the broader scale of climatic-stratigraphic units, *P. auritus* was the most common in pre-glaciation and deglaciation. *P. auritus* and *P. australis* had similar abundances in the early-glaciation, which was followed by *P. australis* being the most abundant in the LGM. *P. shortridgei* had no trend over these climatic-stratigraphic units. From the climatic reconstruction, this change in dominance between *P. australis* and *P. auritus* indicated that *P. australis* preferred cool, dry, C_3 dominated environments where *P. auritus* preferred warm, wet and C_4 dominated environments. Present day studies on *P. australis* showed that this species has adapted to desert life and obtains its water from its diet, which consists of predominantly seeds, supplemented with vegetable matter and insects (Brandle & Pavey, 2008; Watts, 1983). As *P. auritus* is now extinct, there were no inferences in what its diet or habitat was like, however, from the palaeo-data, its apparent preference for wetter and C_4 dominated environments made it more susceptible to extinction in the Naracoorte region, which most likely underwent further drying during the late Holocene (Bowler & Hamada, 1971). *P. shortridgei* in the present day mainly inhabits dry heathlands that has been recently burnt (5-15 yrs), where their diet consists of seeds, flowers and berries in the summer and stems and leaves of grasses during the winter (Cockburn, 1983; Menkhorst et al., 2008; Watts, 1983). Due to the trends of these three species through climatic change, it can be inferred that these

species are resilient to change in vegetation and habitat, which is supported by Macken and Reed (2014).

Future Studies

The isotope values of fossilised rodent bioapatite in the future could be used to predict the palaeoclimate of older sequences. This has the potential of recreating climatic conditions over extinction events on regional and continent-wide scales, such as the megafauna extinction. By looking at the sequences prior to megafauna extinction, we can investigate whether climate change and habitat change had any effect on this extinction. Future studies of the present day *P. australis* and *P. shortridgei* should be conducted to better understand the fractionation between tooth material bioapatite and source water/diet. Inter-tooth variability should also be examined to determine the isotopic variation between dentine and enamel of fossilised rodent teeth, as well as the effect of predator ingestion to observe any effect of digestive alterations. This would help to better understand stable isotopic signatures of bioapatite, and how it can be used to infer changes in climate and vegetation through time.

CONCLUSION

The isotopic composition of bioapatite from fossilised rodent incisors can be used to predict the palaeovegetation and palaeoclimate in which these individuals lived. The reconstruction made from the isotopic signatures from $\delta^{13}C$ and $\delta^{18}O$ showed that in the south-east of South Australia, pre-glaciation had a C_3 dominated vegetation assemblage within a warmer, drier environment, followed by cooler, drier conditions in the C_4 dominated early glaciation period. The LGM continued to cool, dry climate with a C_3

dominated vegetation assemblage. The deglaciation showed an increase in water availability and an increase of C_4 dominance up until approximately 17 ka where the environment shifted to a more C_3 dominated environment of wetter and drier conditions. The comparison of relative abundance and climatic change over the last 50 ka showed that *P. auritus* preferred a warmer, wetter, more C_4 dominated environment whereas *P. australis* preferred a cool, dry, more C_3 dominated environment.

Expanding this study to other cave systems of varying ages in the NCWHA, could help build a better context for climate variability from the middle Pleistocene to Holocene in south-eastern Australia. This could extend into the research of the effects of climate change on the megafauna extinction, as well as the effect of the megafauna extinction on the vegetation, due to the loss of large browsing and grazing herbivores.

ACKNOWLEDGMENTS

I would like to acknowledge the time and efforts made by Dr. Jonathan Tyler, Dr. Francesca McInerney and Dr. Liz Reed, my supervisors throughout the year. The knowledge that they have passed on has allowed me to complete this study. This study was funded by the University of Adelaide, Department of Earth Sciences and I would like to thank them for this contribution. I would like to thank Dr. Mary-Anne Binne (South Australian Museum) for supplying the fossil material for this study. I would like to also thank Sarah McDonald and Alexander Harland, Jonathan Tyler's other honours students for their help and support. Jake Andrae and Jessie-Briar Treloar also helped thoroughly, particularly with my lab work, and I would like to thank them for their assistance. Thank you to Kristine Neilson for assistance in the lab and running my samples. I would like to also thank my fellow honours students who provided insightful comments on the project and moral support.

REFERENCES

ANDRAE, J. W., MCINERNEY, F. A., POLISSAR, P. J., HOWARD, S., HALL, P. A., & PHELPS, S. R. (2018). Initial expansion of C_4 vegetation in Australia during the Late Pliocene. *Geophysical Research Letters, 45*. doi:10.1029/2018GLO77833

BARHAM, M., BLYTH, A. J., WALLWORK, M. D., JOACHIMSKI, M. M., MARTIN, L., EVANS, N. J., . . . MCDONALD, B. J. (2017). Digesting the data- Effects of predator ingestion on the oxygen isotopic signature of micro-mammal teeth. *Quaternary Science Reviews, 176*, 71-84. doi:10.1016/j.quascirev.2017.10.004

BOWLER, J. M., & HAMADA, T. (1971). Late Quaternary stratigraphy and radiocarbon chronology of water level fluctuations in Lake Keilambete, Victoria. *Nature, 239*(5309), 330. doi:10.1038/232330a0

BRANDLE, R., & PAVEY, C. R. (2008). Plains Mouse In S. V. Dyke & R. Strahan (Eds.), *The Mammals of Australia* (3rd ed., pp. 616-618). Australia: Reed New Holland.

BROOKMAN, T. H., & AMBROSE, S. H. (2012). Seasonal variation in kangaroo tooth enamel oxygen and carbon isotopes in southern Australia *Quaternary Research, 78*, 256-265. doi:10.1016/j.yqres.2012.05.011

BROOKMAN, T. H., & AMBROSE, S. H. (2013). Kangaroo tooth enamel oxygen and carbon isotope variation on a latitudinal transect in southern Australia: implications for palaeoenvironmental reconstruction. *Oecologia, 171*, 403-416. doi:10.1007//s00442-012-2425-6

BUILTH, H., KERSAW, P. A., WHITE, C., ROACH, A., HARTNEY, L., MCKENZIE, M., . . . JACOBSEN, G. (2008). Environmental and cultural change on the Mt Eccles lava-flow landscape of southwest Victoria, Australia *The Holocene, 18*(3), 413-424. doi:10.1177/0959683607087931

CERLING, T. E., ANDANJE, S. A., BLUMENTHAL, S. A., BROWN, F. H., CHRITZ, K. L., HARRIS, J. M., . . . UNO, K. T. (2015). Dietary changes of large herbivores in the Turkana Basin, Kenya from 4 to 1 Ma. *PNAS, 112*(37), 11467-11472. doi:10.1073/pnas.1513075112

CERNUSAK, L. A., TCHERKEZ, G., KEITEL, C., CORNWELL, W. K., SANTIAGO, L. S., KNOHL, A., . . . WRIGHT, I. J. (2009). Why are non-photosynthetic tissues generally ^{13}C enriched compared with leaves in C_3 plants? Review and synthesis of current hypotheses. *Functional Plant Biology, 39*(3), 199-213. doi:10.1071/FP08216

CLEMENTZ, M. T. (2012). New insight from old bones: stable isotope analysis of fossil mammals. *Journal of Mammalogy, 93*(2), 368-380. doi:10.1644/11-MAMM-S-179.1

COCKBURN, A. (1983). Heath Rat. In R. Strahan (Ed.), *The Mammals of Australia* (2nd ed., pp. 617-618). Australia: Reed New Holland.

DARRÉNOUGUÉ, N., DE DECKER, P., FITZSIMMONS, K. E., NORMAN, M. D., REED, L., KAARS, S. V. D., & FALLON, S. (2009). A late Pleistocene record of aeolian sedimentation in Blanche Cave, Naracoorte, South Australia. *Quaternary Science Reviews, 28*(25), 2600-2615. doi:10.1016/j.quascirev.2009.05.021

DODSON, J. (1977). Late Quaternary palaeoecology of Wyrie Swamp, southeastern South Australia *Quaternary Research, 8*, 97-114. doi:10.1016/0033-5894(77)90058-8

EDWARDS, E. J., OSBORNE, C. P., STRÖMBERG, C. A. E., SMITH, S. A., & CONSORTIUM, C. G. (2010). The origins of C4 grasslands: integrating evolutionary and ecosystem science. *SCIENCE, 328*(5978), 587-591. doi:10.1126/science.1177216

FALSTER, G., TYLER, J., GRANT, K., TIBBY, J., TURNEY, C., LÖHR, S., . . . KERSAW, P. A. (2018). Millennial-scale variability in south-east Australian hydroclimate between 30,000 and 10,000 years ago. *Quaternary Science Reviews, 192*, 106-122. doi:10.1016/j.quascirev.2018.05.031

FORBES, M. S., & BESTLAND, E. A. (2007). Origin of the sedimentary deposits of the Naracoorte Caves, South Australia. *Geomorphology, 86*, 369-392. doi:10.1016/j.geomorph.2006.09.009

FRANCIS, R. (2017). The plains mouse (*Pseudomys australis*) was declared extinct in Victoria and NSW in the 1990s. In *Australian Geographic*

GEHLER, A., TÜTKEN, T., & PACK, A. (2012). Oxygen and Carbon Isotope Variations in a Modern Rodent Community – Implications for Palaeoenvironmental Reconstructions. *PLOS ONE, 7*(11), e49531. doi:10.1371/journal.pone.0049531

IACUMIN, P., BOCHERENS, H., MARIOTTI, A., & LONGINELLI, A. (1996). Oxygen isotope analyses of co-existing carbonate and phosphate in biogenic apatite: a way to monitor diagenetic alteration of bone phosphate? *Earth and Planetary Science Letters, 142*, 1-6. doi:10.1016/0012-821X(96)00093-3

JOHNSON, B. J., MILLER, G. H., FOGEL, M. L., & BEAUMONT, P. B. (1997). The determination of late Quaternary paleoenvironments at Equus Cave, South Africa, using stable isotopes and amino acid racemization in ostrich eggshell. *Palaeogeography, Palaeoclimatology, Palaeoecology, 136*, 121-137. doi:10.1016/S0031-0182(97)00043-6

KOCH, P. L., TUROSS, N., & FOGEL, M. L. (1997). The Effects of Sample Treatment and Diagenesis on the Isotopic Integrity of Carbonate in Biogenic Hydroxylapatite. *Journal of Archaeological Science, 24*(5), 417-429. doi:10.1006/jasc.1996.0126

LOPES DOS SANTOS, R. A., DE DECKER, P., HOPMANS, E. C., MAGEE, J. W., METS, A., SINNINGHE DAMSTE, J. S., & SCHOUTEN, S. (2013). Abrupt vegetation change after the late Quaternary megafaunal extinction in southeastern Australia. *NATURE GEOSCIENCE, 6*, 627-631. doi:10.1038/NGEO1856

LOPES DOS SANTOS, R. A., WILKINS, D., DECKER, P. D., & SCHOUTEN, S. (2012). Late Quaternary productivity changes from offshore southeastern Australia: a biomarker approach. *Palaeogeography, Palaeoclimatology, Palaeoecology, 363-364*, 48-56. doi:10.1016/j.palaeo.2012.08.013

MACKEN, A. C., PRIDEAUX, G. J., & REED, E. H. (2012). Variation and pattern in the responses of mammal faunas to Late Pleistocene climatic change in southeastern South Australia. *Journal of Quaternary Science, 27*(4), 415-424. doi:10.1002/jqs.1563

MACKEN, A. C., & REED, E. H. (2013). Late Quaternary small mammal faunas of the Naracoorte Caves World Heritage Area *Royal Society of South Australia, 137*(1), 53-67. doi:10.1080/3721426.2013.10887171

MACKEN, A. C., & REED, E. H. (2014). Postglacial reorganization of a small-mammal paleocommunity in southern Australia reveals thresholds of change. *Ecological Society of America, 84*(4), 563-577. doi:10.1890/13-0713.1

MACKEN, A. C., STAFF, R. A., & REED, E. H. (2013). Bayesian age-depth modelling of Late Quaternary deposits from Wet and Blanche Caves, South Australia: A framework for comparative faunal analyses. *quaternary Geochronology, 17*, 26-43. doi:10.1016/j.quageo.2013.03.001

MEERBEECK, C. J. V., VAN MEERBEECK, C. J., RENSSEN, H., & ROCHE, D. M. (2009). How did marine isotope stage 3 and last glacial maximum climates differ? - perspectives from equilibrium simulations. *Climate of the Past, 5*, 33-51.

MENKHORST, P. W., COCKBURN, A., & CANCILLA, D. (2008). Heath Mouse. In S. V. Dyke & R. Strahan (Eds.), *The Mammals of Australia* (3rd ed., pp. 650-652). Australia: Reed New Holland.

MILLER, G. H., FOGEL, M. L., MAGEE, J. W., GAGAN, M. K., CLARK, S. J., & JOHNSON, B. J. (2005). Ecosystem Collapse in Pleistocene Australia and a Human Role in Megafaunal Extinction. *SCIENCE, 309*(5732), 287-290.

MONTANARI, S., LOUYS, J., & PRICE, G. J. (2013). Pliocene paleoenvironments of southeastern Queensland, Australia inferred from stable isotopes of marsupial tooth enamel. *PLOS ONE, 8*(6), e66221. doi:10.1371/journal.pone.0066221

PASSEY, B. H., & CERLING, T. E. (2002). Tooth enamel mineralization in ungulates: Implications for recovering a primary isotopic time-series. *Geochimica et Cosmochimica Acta, 66*(18), 3225-3234. doi:10.1016/S0016-7037(02)00933-X

PAUL, D. (2017). Heath Rat, *Pseudomys shortridgei*. Grampians National Park, Victoria. In. Museums Victoria.

PEDRO, J. B., VAN OMMEN, T., RASMUSSEN, S. O., MORGAN, V. I., CHAPPELLAZ, J., MOY, A. D., . . . DELMOTTE, M. (2011). The last deglaciation: timing the bipolar seesaw. *Climate of the Past, 7*, 671-683. doi:10.5194/cp-7-671-2011

PETHERICK, L., BOSTOCK, H., COHEN, T. J., FITZSIMMONS, K., TIBBY, J., FLETCHER, M.-S., . . . DOSSETO, A. (2013). Climatic records over the past 30 ka from temperate Australia - a synthesis from the Oz-INTIMATE workgroup. *Quaternary Science Reviews, 74*, 58-77. doi:10.1016/j.quascirev.2012.12.012

PRIDEAUX, G. J., ROBERTS, R. G., MEGIRIAN, D., WESTAWAY, K. E., HELLSTORM, J. C., & OLLEY, J. M. (2007). Mammalian response to Pleistocene climate change in southeastern Australia. *Geological Society of America, 35*(1), 33-36. doi:10.1130/G23070A.1

QUINN, R. L. (2010). Geology and Anthropology. In H. J. Brix (Ed.), 21st Century Anthropology: A Reference Handbook (pp. 388-397). Thousand Oaks: SAGE Publications, Inc. doi:10.4135/9781412979283.n40

REED, E. H., & BOURNE, S. J. (2000). Pleistocene fossil vertebrate sites of the south-eastern region of South Australia. *Transactions of the Royal Society of South Australia, 124*(2), 61-90.

REEVES, J. M., BARROWS, T. T., COHEN, T. J., KIEM, A. S., BOSTOCK, H. C., FITZSIMMONS, K. E., . . . MEMBERS, O.-I. (2013). Climate variability over the last 35,000 years recorded in marine and terrestrial archives in the Australian region: an OZ-INTIMATE compilation *Quaternary Science Reviews, 74*, 21-34. doi:10.1016/j.quascirev.2013.01.001

ROBERTS, R. G., FLANNERY, T. F., AYLIFFE, L. K., YOSHIDA, H., OLLEY, J. M., PRIDEAUX, G. J., . . . SMITH, B. L. (2001). New Ages for the Last Australian Megafauna: Continent-Wide

Extinction About 46,000 Years Ago. *SCIENCE, 292*(5523), 1888-1892. doi:10.1126/science.1060264

ROBU, M., FORTIN, J. K., RICHARDS, M. P., SCHWARTS, C. C., WYNN, J. G., ROBBINS, C. T., & TRINKAUS, E. (2013). Isotopic evidence for dietary flexibility among European Late Pleistocene cave bears (*Ursus spelaeus*). *Canadian Journal of Zoology, 91*, 227-234. doi:10.1139/cjz-2012-0222

ROBU, M., WYNN, J. G., MIREA, I. C., PETCULESCU, A., KENESZ, M., PUŞCAŞ, C. M., . . . CONSTANTIN, S. (2017). The diverse dietary profiles of MIS 3 cave bears from the Romanian Carpathians: insights from stable isotope (δ13 and δ15) analysis. *Palaeontology, 61*(2), 209-219. doi:10.1111/pala.12338

SALTRÉ, F., RODRÍGUEZ-REY, M., BROOK, B. W., JOHNSON, C. N., TURNEY, C. S. M., ALROY, J., . . . BRADSHAW, C. J. A. (2016). Climate change not to blame for late Quaternary megafauna extinctions in Australia. *Nature Communications, 7*, 1-7. doi:10.1038/ncomms10511

ST PIERRE, E., ZHAO, J.-X., FENG, Y.-X., & REED, E. (2012). U-series dating of soda straw stalactites from excavated deposits: method development and application to Blanche Cave, Naracoorte, South Australia. *Journal of Archaeological Science, 39*, 922-930. doi:10.1016/j.jas.2011.10.027

TRALYER, R. B., & KOHN, M. J. (2017). Tooth enamel maturation reequilibrates oxygen isotope composition and supports simple sampling methods. *Geochimica et Cosmochimica Acta, 198*, 32-47. doi:10.1016/j.gca.2016.10.023

TRUEMAN, C. N. G., FIELD, J. H., DORTCH, J., CHARLES, B., & WROE, S. (2005). Prolonged coexistance of humans and magefauna in Pleistocene Australia *PNAS, 102*(23), 8381-8385.

TURNEY, C. S. M., HABERLE, S., FINK, D., KERSHAW, A. P., BARBETTI, M., BARROWS, T. T., . . . XIA, Q. (2006). Integration of ice-core, marine and terrestrial records for the Australian Last Glacial Maximum and Termination: a contribution from the OZ INTIMATE group. *Journal of Quaternary Science, 21*(7), 751-761. doi:10.1002/jqs.1073

WATTS, C. H. S. (1983). Plains Rat. In R. Strahan (Ed.), *The Mammals of Australia* (2nd ed., pp. 586-587). Australia: Reed New Holland.

WHITE, S., & WEBB, J. A. (2015). The influence of tectonics on flank margin cave formation on a passive continental margin: Naracoorte, Southeastern Australia. *Geomorphology, 229*, 58-72. doi:10.1016/j.geomorph.2014.09.003

WILLIAMS, N. J., HARLE, K. J., GALE, S. J., & HEIJNIS, H. (2006). The vegetation history of the last glacial-interglacial cycle in eastern New South Wales, Australia. *Journal of Quaternary Science, 21*(7), 735-750. doi:10.1002/jqs

APPENDIX A: LABORATORIAL METHODS

Relative abundance

- For each layer, the left and right lower jaws (dentaries) were counted and recorded for each species.
- The minimum number of individuals (MNI) was calculated using the most abundant dentary side for each species over the sequence.
- The number of specimens (NISP) was calculated using all dentaries for each species over the sequence.

Collection of incisors

- The layers that had 5 or more dentaries that were in good condition, had no serious damage or chemical alteration through digestion or magnesium alterations and had incisors were used to sample.
- The jaws were re-identified using the Rodents of Australia Book by C.H.S Watts and H.J Aslin. Help for the identification was also given by Jessie-Briar Treloar.
- Between 5 and 15 teeth were sampled with the jaw being photographed before and after the teeth were extracted.
- The jaws that were sampled were placed by layers and species in tubes to be later registered to the South Australian Museum.

Preparation of the teeth

1. The teeth were crushed into a fine powder using an agate mortar and pestle. Between samples, the mortar and pestle was cleaned with methanol to ensure that there were no contaminations from the previous sample. Methanol was used as it dries fast.
2. Once the samples were crushed the sample powder was weighed to determine the total sample weight.

Pre-treatment of the teeth

1. Approximately 20 mg of sample was weighed out into a 1.5 mL centrifuge tube.
2. The sample was reacted with 1 ml of 30 % hydrogen peroxide for 24 hours (the lid of the centrifuge tube was left open with a piece of paper towel over the top to stop contaminants entering. The tubes were left in a fume hood over the reaction period).
3. The sample was then centrifuged and rinsed 5 times (centrifuged, pipette off supernatant, add 1 mL of reverse osmosis water (RO water), agitate and repeat).
4. 1 mL of 1 M calcium acetate buffer solution was added and left to react for an additional 24 hours. (The lid of the centrifuge tube was left open with a piece of paper towel over the top to stop contaminates entering. The tubes were left in a fume hood over the reaction period).
    - 1 M calcium acetate buffer solution was made by combining 8.8 g of calcium acetate powder with 3 mL of acetic acid. The remaining volume was made up by RO water (50 mL of water) this gave a solution that was at pH 5 which was suggested in the Gehler et al (2012).

5. The sample was then centrifuged and rinsed 5 times (centrifuged, pipette off supernatant, add 1mL of RO water, agitate and repeat).
6. Once rinsed the samples were placed in a 50ºC oven with the tops of the centrifuge tube open, for 24 hours or until the powder is dry. (As the lids were open the samples were placed on the top shelf to avoid any contaminates from entering the tubes).

Carbonate method

1. Approximately 2 mg of pre-treated sample was placed in a clean mass spec tube
2. Standards of P3, UAC and CO8 were weighed out it various weights to normalise sample data obtained.
3. The samples were reacted with 100 % phosphoric acid for 15 minutes using a Gas Bench Device that was coupled via continuous flow with a Nu Horizon Isotope Ration Mass Spectrometer (IRMS).

Phosphate method

1. Approximately 1mg of the pre-treated sample was weighed into a 1.5 mL centrifuge tube.
2. 200 μL of 0.5 M nitric acid was added to the sample and allowed to react until the sample was dissolved. (The lid of the centrifuge tube was left open with a piece of paper towel over the top to stop contaminates entering. The tubes were left in a fume hood over the reaction period).
    - The 0.5 M solution was made from 5 M nitric acid by combining 1 mL of 5 M nitric acid in 9 mL of RO water.
    - The sample was completely dissolved after approximately 12 hours. The solution was clear.
3. 150 μL of 0.5 M potassium hydroxide was added to the solution. This is to neutralise the solution.
    - The 0.5 M solution was made by adding approximately 0.2116 g of KOH powder to approx. 7.5 mL of RO water.
    - As the solution is neutralised the next step could be performed straight after. However, due to a lack of time to prepare the next solution, the next step was performed approx. 12 hours later.
4. 400 μL of 0.36 M potassium fluoride was added to the solution to produce a precipitate of calcium fluoride. This solution was left to react for approximately 3 hours. (The lid of the centrifuge tube was left open with a piece of paper towel over the top to stop contaminates entering. The tubes were left in a fume hood over the reaction period).
    - The precipitate did not form immediately but after about 1 hour. The solution was then left for another 2 hours to ensure that no more precipitate would form. The precipitate was approximately the size of the original sample powder.
    - The 0.36 M solution of KF was made by combining approximately 0.4191 g of KF powder with approximately 20 mL of RO water.

5. The tubes were centrifuged and then the supernatant was removed and placed into a clean centrifuge tube. The resulting precipitate from the previous step was left in the original tube and discarded.
    - The supernatant was a clear solution.
6. 500 μL of silver amine solution was added to the centrifuge tube and placed in an oven at approximately 30ºC overnight.
    - The silver amine solution was made by combining the following chemicals.
        - 0.85031 g of silver nitrate powder.
        - 0.70085 g of ammonium nitrate powder.
        - 41 μL of ammonium hydroxide (ammonia solution at 30 %).
        - Approx. 25 mL of RO water.
    - The solution was made in a 50 ml centrifuge tube by adding the silver nitrate and ammonium nitrate to the ammonium hydroxide and then adding the water (there was no reaction when the chemicals were combined but when the water was added, the solution went from clear to a milky/cloudy white).
    - When the silver amine solution was added to the supernatant solution, that was clear, the whole solution turned a cloudy yellow colour.
    - After a night in the oven, there was a thick greenish yellow precipitate at the bottom of the tube. Some of the precipitate had formed on the side of the tubes. There also seemed to be no reduction in the amount of solution in the tubes (no evaporation of the solution).
    - There were different amounts of the precipitate over the samples but they all had the same colour and consistency.
7. The solution was then centrifuged and the supernatant removed. The precipitate was then rinsed 5 times (centrifuged, pipette off supernatant, add 1 mL of RO water, agitate and repeat).
    - The yellow grime that was on the side of the tubes would not come off the side no matter how long it was in the centrifuge
8. The leftover precipitate was then placed in the oven at 30ºC overnight to allow to dry.
    - Being in the oven overnight was enough time for the precipitate to be dried. However there didn't seem to be any visible crystal in any of the tubes, it looks more like a powder then crystals.
    - The colour of the precipitate did not change after being dried. However, the side grime seemed to become more reddish-orange than yellow in some of the tubes.
9. The resulting crystals were observed under a microscope.
    - Under the microscope, there were small black to dark green clumps of dried precipitate.
    - When the clumps were moved around they broke up quite easily.
    - There were no visible crystals, however, there were flecks of reflecting light which would indicate that there was crystalline material.
10. Approximately 0.5 mg of powder was weighed into silver cup.

11. The standards were keratin (Kudu Horn (KHS), and Caribou Hoof (CBS)), IAEA-NO-3, NBS-127 and USGA-32. They were weighed out it various weights to normalise sample data obtained.
12. The samples were run by a high temperature conversion isotope mass spectrometry using an Elemantar high temperature pyrolysis furnace coupled via continuous flow to a Nu Horizon mass spectrometer.

APPENDIX B: ISOTOPE DATA

Table 1: Table of results for *Pseudomys auritus* displaying all isotopic data obtained from the incisors from Blanche Cave, Naracoorte Caves World Heritage Area (NCWHA), south-eastern South Australia

	Pseudomys auritus				
Layer No.	No. Teeth analysed	$\delta^{13}C_{tooth}$(‰)	$\delta^{13}C_{diet}$(‰)	$\delta^{18}O_{CO3}$(‰)	$\delta^{18}O_{PO4}$(‰)
1					
2					
3	10	-10.4919	-22.4759	0.213249	23.4
4	10	-10.962	-22.951	-0.25585	21.3
5	10	-11.4593	-23.4541	-1.35014	22.6
6	15	-10.7185	-22.7049	0.827574	22.4
7	10	-11.1317	-23.1227	0.215255	21.9
8	10	-11.2744	-23.267	-0.61351	21.4
9					
10	15	-10.7863	-22.7735	-0.32807	22.7
11	10	-10.6598	-22.6456	-1.20375	21.7
12					
13	5	-9.04289	-21.0126	0.342323	23
14					
15		-10.8824	-22.8706	-0.47797	22.7
16					
17	5				
18					
19	5	-7.92809	-19.8883	1.853063	24.2
20					
21					
22	10	-7.51692	-19.4739	0.741872	22.4
23	10	-8.47887	-20.4436	1.277939	24
24	15	-9.31483	-21.2871	-0.05311	21.6
25	15	-9.2729	-21.2447	0.517259	22.9
26	15	-10.0817	-22.0614	0.484563	23.4
27	6	-9.56021	-21.5348	0.619167	23.5

Table 2: Table of results for *Pseudomys australis* displaying all isotopic data obtained from the incisors from Blanche Cave, Naracoorte Caves World Heritage Area (NCWHA), south-eastern South Australia

	Pseudomys australis				
Layer No.	No. Teeth analysed	$\delta^{13}C_{tooth}$(‰)	$\delta^{13}C_{diet}$(‰)	$\delta^{18}O_{CO3}$(‰)	$\delta^{18}O_{PO4}$(‰)
1					
2					
3	10	-11.8773	-23.877	-0.11142	21.1
4	10	-11.3777	-23.3715	0.244334	22.5
5					
6	10	-10.0417	-22.021	1.134838	22.9
7	6	-10.7643	-22.7512	0.433064	22.2
8	10	-9.7522	-21.7286	-0.00523	21.5
9	5	-11.4826	-23.4776	-4.93225	23.1
10	15	-10.6271	-22.6126	0.677678	22.9
11	10	-10.2	-22.1809	0.182289	22
12					
13	10	-9.84746	-21.8248	0.309225	22.8
14					
15	5	-11.659	-23.656	0.750341	23.1
16					
17	15	-11.4026	-23.3967	-0.15461	22.7
18					
19	10	-8.19509	-20.1574	1.208909	22.9
20					
21					
22	10	-8.22612	-20.1887	1.144148	22.8
23	5	-8.73089	-20.6978	0.341116	21.9
24	15	-9.00213	-20.9715	1.00647	22.7
25	8	-11.0235	-23.0133	-0.09692	21.7
26	15	-10.5112	-22.4954	0.762526	22.3
27	7	-9.44201	-21.4154	-0.29962	21.3

Table 3: Table of results for *Pseudomys shortridgei* displaying all isotopic data obtained from the incisors from Blanche Cave, Naracoorte Caves World Heritage Area (NCWHA), south-eastern South Australia

	Pseudomys shortridgei				
Layer No.	No. Teeth analysed	$\delta^{13}C_{tooth}$(‰)	$\delta^{13}C_{diet}$(‰)	$\delta^{18}O_{CO3}$(‰)	$\delta^{18}O_{PO4}$(‰)
1					
2					
3	10	-10.7053	-22.6915	-1.82404	22.1
4					
5					
6					
7					
8					
9					
10	10	-8.44676	-20.4112	-1.09025	22.5
11					
12					
13					
14					
15					
16					
17	9	-10.618	-22.6033	-0.34239	23.5
18					
19					
20					
21					
22	10	-6.58507	-18.5354	-0.59725	22.6
23					
24					
25					
26	10	-8.262	-20.2249	-0.66198	21.9
27					

APPENDIX C: RELATIVE ABUNDANCE DATA

Table 4: Table of results showing a dentary count for each species throughout all layers differentiating between left and right dentary.

	Dentary Count For Relative Abundance					
	P. auritus		*P. australis*		*P. shortridgei*	
Layer	Left	Right	Left	Right	Left	Right
1	3	2	5	3	2	1
2	0	0	0	0	0	0
3	12	7	8	8	7	6
4	12	13	7	6	9	6
5	12	9	2	8	7	5
6	12	16	9	14	4	6
7	7	9	5	3	7	5
8	21	15	6	12	6	7
9	4	2	1	5	0	3
10	14	18	12	10	7	9
11	12	9	5	8	5	7
12	0	0	0	0	0	0
13	5	7	8	7	4	2
14	0	1	0	4	1	2
15	5	1	5	3	2	3
16	0	2	0	7	2	0
17	0	11	3	14	5	9
18	0	1	0	3	1	1
19	6	2	9	14	2	2
20	0	0	1	2	0	0
21	2	0	1	0	1	2
22	12	13	3	12	10	8
23	12	2	7	10	3	2
24	18	33	28	31	19	15
25	65	70	14	9	23	12
26	106	132	55	47	59	71
27	8	7	1	10	1	2

Table 5: Table showing the dentary count of each of the three species of *Pseudomys* across the first 27 layers of the Blanche Cave excavation site in Naracoorte, South Australia. The minimum number of individuals (MNI) and the number of specimens (NISP) were counted.

	Relative Abundance					
	P. auritus		*P. australis*		*P. shortridgei*	
Layer	MNI	NISP	MNI	NISP	MNI	NISP
1	3	5	5	8	2	3
2	0	0	0	0	0	0
3	12	19	8	16	7	13
4	13	25	7	13	9	15
5	12	21	8	10	7	12
6	16	28	14	23	6	10
7	9	16	5	8	7	12
8	21	36	12	18	7	13
9	4	6	5	6	3	3
10	18	32	12	22	9	16
11	12	21	8	13	7	12
12	0	0	0	0	0	0
13	7	12	8	15	4	6
14	1	1	4	4	2	3
15	5	6	5	8	3	5
16	2	2	7	7	2	2
17	11	11	14	17	9	14
18	1	1	3	3	1	2
19	6	8	14	23	2	4
20	0	0	2	3	0	0
21	2	2	1	1	2	3
22	13	25	12	15	10	18
23	12	14	10	17	3	5
24	33	51	31	59	19	34
25	70	135	14	23	23	35
26	132	238	55	102	71	130
27	8	15	10	11	2	3

Table 6: Table showing the dentary count of each of the three species of *Pseudomys* across the first 27 layers of the Blanche Cave excavation site in Naracoorte, South Australia. The NISP values for the three species are displayed, as well as the total NISP value for all 27 layers.

	NISP Relative Abundance			
Layer	*P. auritus*	*P. australis*	*P. shortridgei*	Total
1	5	8	3	16
2	0	0	0	0
3	19	16	13	48
4	25	13	15	53
5	21	10	12	43
6	28	23	10	61
7	16	8	12	36
8	36	18	13	67
9	6	6	3	15
10	32	22	16	70
11	21	13	12	46
12	0	0	0	0
13	12	15	6	33
14	1	4	3	8
15	6	8	5	19
16	2	7	2	11
17	11	17	14	42
18	1	3	2	6
19	8	23	4	35
20	0	3	0	3
21	2	1	3	6
22	25	15	18	58
23	14	17	5	36
24	51	59	34	144
25	135	23	35	193
26	238	102	130	470
27	15	11	3	29

Table 7: Table showing the NISP relative abundance (%) of the three *Pseudomys* species of the first 27 layers of the Blanche Cave Excavation site Naracoorte, South Australia.

	NISP Relative Abundance (%)		
Layer	*P. auritus*	*P. australis*	*P. shortridgei*
1	31.25	50	18.75
2	0	0	0
3	39.58333	33.33333	27.08333
4	47.16981	24.5283	28.30189
5	48.83721	23.25581	27.90698
6	45.90164	37.70492	16.39344
7	44.44444	22.22222	33.33333
8	53.73134	26.86567	19.40299
9	40	40	20
10	45.71429	31.42857	22.85714
11	45.65217	28.26087	26.08696
12	0	0	0
13	36.36364	45.45455	18.18182
14	12.5	50	37.5
15	31.57895	42.10526	26.31579
16	18.18182	63.63636	18.18182
17	26.19048	40.47619	33.33333
18	16.66667	50	33.33333
19	22.85714	65.71429	11.42857
20	0	100	0
21	33.33333	16.66667	50
22	43.10345	25.86207	31.03448
23	38.88889	47.22222	13.88889
24	35.41667	40.97222	23.61111
25	69.94819	11.9171	18.13472
26	50.6383	21.70213	27.65957
27	51.72414	37.93103	10.34483

Table 8: Table showing the dentary count of each of the three species of *Pseudomys* across the first 27 layers of the Blanche Cave excavation site in Naracoorte, South Australia. The MNI values for the three species are displayed, as well as the total MNI value for all 27 layers.

	MNI Relative Abundance			
Layer	*P. auritus*	*P. australis*	*P. shortridgei*	Total
1	3	5	2	10
2	0	0	0	0
3	12	8	7	27
4	13	7	9	29
5	12	8	7	27
6	16	14	6	36
7	9	5	7	21
8	21	12	7	40
9	4	5	3	12
10	18	12	9	39
11	12	8	7	27
12	0	0	0	0
13	7	8	4	19
14	1	4	2	7
15	5	5	3	13
16	2	7	2	11
17	11	14	9	34
18	1	3	1	5
19	6	14	2	22
20	0	2	0	2
21	2	1	2	5
22	13	12	10	35
23	12	10	3	25
24	33	31	19	83
25	70	14	23	107
26	132	55	71	258
27	8	10	2	20

Table 9: Table showing the MNI relative abundance (%) of the three *Pseudomys* species of the first 27 layers of the Blanche Cave Excavation site Naracoorte, South Australia.

	MNI Relative Abundance (%)		
Layer	*P. auritus*	*P. australis*	*P. shortridgei*
1	30	50	20
2	0	0	0
3	44.44444	29.62963	25.92593
4	44.82759	24.13793	31.03448
5	44.44444	29.62963	25.92593
6	44.44444	38.88889	16.66667
7	42.85714	23.80952	33.33333
8	52.5	30	17.5
9	33.33333	41.66667	25
10	46.15385	30.76923	23.07692
11	44.44444	29.62963	25.92593
12	0	0	0
13	36.84211	42.10526	21.05263
14	14.28571	57.14286	28.57143
15	38.46154	38.46154	23.07692
16	18.18182	63.63636	18.18182
17	32.35294	41.17647	26.47059
18	20	60	20
19	27.27273	63.63636	9.090909
20	0	100	0
21	40	20	40
22	37.14286	34.28571	28.57143
23	48	40	12
24	39.75904	37.3494	22.89157
25	65.42056	13.08411	21.49533
26	51.16279	21.31783	27.51938
27	40	50	10

Table 10: Table showing the dentary count of each of the three species of *Pseudomys* across the first 27 layers of the Blanche Cave excavation site in Naracoorte, South Australia. The MNI and NISP values for the three species are displayed, as well as the total MNI and NISP value for the whole sequence.

	Relative Abundance Total			
	P. auritus	*P. australis*	*P. shortridgei*	Total
MNI	423	274	217	914
NISP	730	445	373	1548

Table 11: Table showing the MNI and NISP relative abundance (%) of the three *Pseudomys* species of the whole sequence of the Blanche Cave Excavation site Naracoorte, South Australia.

	Relative Abundance Total (%)	
	NISP	MNI
P. auritus	47.15762	46.28009
P. australis	28.74677	29.97812
P. shortridgei	24.09561	23.74179

Table 12: Table showing the dentary count of each of the three species of *Pseudomys* across the climatic-stratigraphic units of the Blanche Cave excavation site in Naracoorte, South Australia. The NISP values for the three species are displayed, as well as the total NISP value for each climatic-stratigraphic units.

	NISP Relative Abundance			
Units	*P. auritus*	*P. australis*	*P. shortridgei*	Total
4	221	152	115	488
3	28	58	27	113
2	92	95	60	247
1	388	136	168	692

Table 13: Table showing the NISP relative abundance (%) of the three *Pseudomys* species of the climatic-stratigraphic units of the Blanche Cave Excavation site Naracoorte, South Australia.

	NISP Relative Abundance (%)		
Units	*P. auritus*	*P. australis*	*P. shortridgei*
4	45.28688525	31.14754098	23.56557377
3	24.77876	51.32743	23.89381
2	37.24696	38.46154	24.2915
1	56.06936	19.65318	24.27746

Table 14: Table showing the dentary count of each of the three species of *Pseudomys* across the climatic-stratigraphic unit of the Blanche Cave excavation site in Naracoorte, South Australia. The MNI values for the three species are displayed, as well as the total MNI value for each climatic-stratigraphic unit.

	MNI Relative Abundance			
Units	*P. auritus*	*P. australis*	*P. shortridgei*	Total
4	127	92	68	287
3	25	43	17	85
2	60	56	34	150
1	210	79	96	385

Table 15: Table showing the MNI relative abundance (%) of the three *Pseudomys* species of the climatic-stratigraphic units of the Blanche Cave Excavation site Naracoorte, South Australia.

	MNI Relative Abundance (%)		
Units	*P. auritus*	*P. australis*	*P. shortridgei*
4	44.25087108	32.05574913	23.69337979
3	29.41176	50.58824	20
2	40	37.33333	22.66667
1	54.54545	20.51948	24.93506